Submission to [Mater. Sci. & Eng. A]

Real-time ultrasonic measurement during tensile testing of aluminum alloys

Xiao-Hua Min [1], Hiroshi Kato [2], Nobuyuki Narisawa[2] and Kensuke Kageyama[2]

1 Graduate School of Science and Engineering, Saitama University, 255 Shimo-Okubo, Sakura-ku, Saitama 338-8570, Japan

2 Department of Mechanical Engineering, Faculty of Engineering, Saitama University, 255 Shimo-Okubo, Sakura-ku, Saitama 338-8570, Japan

ABSTRACT

A real-time ultrasonic measurement was carried out for aluminum alloy (A2024-T3) specimens during tensile testing with local immersion method by using a water bag to obtain ultrasonic parameters. The sound velocity increased with increasing strain in the elastic deformation, and then decreased with increasing plastic strain during tensile testing. From a relation between the sound velocity and the elastic strain, the acousto-elastic constant was calculated to be 8.5×10^{-6} MPa^{-1}. The surface roughness and the hardness were measured for specimens taken out from testing machine after required strain. The peak intensity of the bottom echo spectrum and the average gradient of the transfer function (AGTF) obtained from the bottom echo spectrum decreased with increasing plastic strain. The decrease in the ultrasonic parameters was explained from the change in the dislocation density and arrangement by using Granato and Lücke string model. The peak frequency of the bottom echo spectrum did not change with increasing plastic strain. The ultrasonic parameters were measured off-line with specimens taken out from testing machine after required strain by the conventional immersion method, and decreased with increasing plastic strain as those obtained in real-time. When specimens were annealed, the hardness continuously decreased with increasing annealing time, and the yield strength and the sound velocity slightly increased after smaller annealing time, and then decreased with increasing annealing time. For annealed specimens, the peak intensity and AGTF obtained by the real-time measurement also decreased with increasing plastic strain, and the rates of the ultrasonic parameters increased with increasing annealing time.

Key words: Ultrasonic parameters, Real-time measurement, Plastic strain, Annealing treatment, Dislocation density and arrangement.

1. Introduction

When materials are subjected to an external load, degradation occurs in materials to result in final failure, and many researches have been carried out on degradation and damaging processes of materials for avoidance of final failure. Among mechanical properties, static tensile properties are most fundamental and related to other mechanical properties, and have been used as a standard to represent mechanical properties. When materials deform, elastic deformation occurs in an early stage. When the deformation proceeds and exceeds a critical value, it becomes plastic, and the dislocation density increases. In such a manner, tensile properties have a close relation to the dislocation density and arrangement, and hence these have been crucial for quantitative discussion of plastic deformation process. So far, for quantitative examination of dislocations, TEM observation has been utilized with a thin foil made of tensile specimens. In recent years, the quantitative analysis of the lattice spacing by using the X-ray diffraction method has been developed for estimation of the dislocation density and arrangement [1]. Since these analyses are not carried out in real-time during tensile testing, but done off-line with specimens taken out from a testing machine after a required strain. If material properties are continuously evaluated in real-time during tensile testing, useful information can be obtained on the damaging process of materials.

As the X-ray, the ultrasonic wave is also sensitive to microstructures of materials. As early as 1950's, Granato and Lücke [2,3] had discussed on changes in ultrasonic attenuation and velocity with dislocation mobility by using the string model, namely dislocation damping theory. In the last decade, many researchers have focused their attention on ultrasonic evaluation of material deformation following Granato and Lücke [4,5,6]. One of authors [7,8], carried out the ultrasonic measurement for plastically deformed brass copper plates, and found that the ultrasonic parameters obtained from the Fourier spectrum of the bottom echo monotonically changed following the plastic deformation. However, in these works [7,8], the ultrasonic measurement was performed off-line for specimens deformed to predetermined strains. In recent years, many monitoring methods were developed to evaluate the microstructural evolution in real-time during deformation [9,10,11]. If the ultrasonic wave is measured in real-time during tensile testing, the ultrasonic parameters can be used as measures to evaluate damaging level of specimen in real-time.

It is well known that the initial state of alloys, such as recovered, recrystallised or cold

worked state, plays an important role in the subsequent microstructural evolution [12]. Liu et al. [13,14] studied the microstructural evolution of Al-3004 being subjected to the tensile testing after a predeformation by rolling, and showed that the predeformation strongly influenced the mechanical behavior of the alloy. Although metallographic and hardness measurements have been widely utilized for characterization of alloys after annealing and deformation, there are distinct requirements for nondestructive characterization of alloys after annealing or deformation. Palanichamy et al. [15] applied the ultrasonic testing to characterize the microstructural evolution during annealing of cold worked titanium modified 316 stainless steel and found a correlation of the sound velocity with microstructures and mechanical properties.

In the present work, a local immersion method of the ultrasonic measurement was carried out by using a water bag to evaluate the deformation process of rolled aluminum alloy (A2024-T3) plates in real-time during tensile testing, and relations between ultrasonic parameters and deformation strain were obtained. Influences of annealing on the ultrasonic parameters were also examined.

2. Material and experimental procedures

2.1 Specimen preparation

Tensile specimens were fabricated from rolled aluminum alloy (A2024-T3) plates to have a gauge length 80 mm, width of 12.5 mm and thickness of 4 mm so that the specimen axis was parallel to the rolling direction. As-received plates were processed through T3 treatment: solution treatment, quenching, cold working, and then natural aging successively. The chemical composition and the mechanical properties of the alloy were shown in the previous work [16]. Some of specimens were annealed at 573 K for 0, 1, 2, 4 and 8 hours before tensile testing.

Specimens were polished and etched with a water solution of sodium hydroxide, and then subjected to microstructure observation through optical microscope.

2.2 Tensile testing

The specimens were subjected to the tensile testing at room temperature with a cross-head

speed of 5 $\times 10^{-3}$mm/s (an initial strain rate of 6.25×10^{-5} in gauge length of 80 mm). Some of specimens were taken out after deformation of required plastic strains and subjected to the ultrasonic measurement, and others were pulled to fracture in conjunction with the real-time ultrasonic measurement.

2.3 Ultrasonic measurement and wave analysis

A setup for real-time ultrasonic measurement is shown in Fig. 1. The ultrasonic measurement was carried out with a local immersion method by using a water bag [16,17,18]. The thickness of the specimen was also measured during the tensile testing by using a micrometer. Some of specimens were taken out from testing machine after required plastic strains, and then subjected to off-line ultrasonic measurement by using the conventional immersion method. A transducer generating a longitudinal wave of 20 MHz in frequency with a focal distance of 25.4 mm in water was used. In the measurement, the water path was controlled to be about 7 mm so that a focal position of the ultrasonic wave was focused on the bottom of the specimen.

A propagation time of the ultrasonic wave reflected from the surface to the bottom was obtained from these echoes to obtain the sound velocity. Bottom echoes were subjected to the FFT analysis to obtain the Fourier spectra. The peak intensity, the peak frequency and the average gradient of the transfer function (AGTF) from the bottom wave spectrum were obtained as shown in the previous work [16].

2.4 Surface roughness and hardness measurements

After the off-line ultrasonic measurement by using the conventional immersion method, specimens were subjected to the surface roughness and the hardness measurements. The surface roughness of the specimen was measured by using the laser surface roughness meter in a range of 10 mm at a center of the specimen. The arithmetic mean value of the surface roughness was obtained for each specimen. The Vickers hardness was measured with a load of 49 N at 10 points for each specimen, and the arithmetic mean value of the hardness was obtained.

3. Results and discussion

3.1 Change in ultrasonic parameters measured off-line with deformation

The ultrasonic waves were measured for specimens taken out from testing machine after required plastic strains by using the conventional immersion method, and then ultrasonic parameters were obtained through the FFT analysis of the bottom echo. Changes in the ultrasonic parameters with deformation strain were obtained as shown in Fig. 2. The peak intensity and AGTF decreased with increasing strain. However, no change of the peak frequency was obtained within the accuracy of the present measurement.

Tensile deformation behavior of the materials is depended on the dislocation density and arrangement, and before necking occurs, dislocations are certainly the major active players. The surface roughness and the hardness were measured for the specimens taken out from testing machine after required plastic strains, and the results were obtained as shown in Fig. 3. From this figure, it was found that the surface roughness and the hardness increased with increasing plastic strain. With increasing plastic strain, the persistent slip bands were formed on the surface of the specimen to increase a roughness on the surface. The hardness increased due to work-hardening caused by increasing dislocation density and tangling of dislocations [13,19]. Therefore, changes in the surface roughness and the hardness with strain were similar.

3.2 Change in ultrasonic parameters measured in real-time with deformation

During tensile testing, the propagation time of ultrasonic wave from the surface to the bottom and the specimen thickness were measured in real-time as shown in Fig. 4. The propagation time slightly decreased before 0.6 % strain under elastic regime, and then, gradually decreased with increasing plastic strain. The specimen thickness decreased slightly before 0.6 % strain, and gradually decreased with increasing plastic strain. From the specimen thickness and the propagation time of the ultrasonic wave, the sound velocity with deformation strain was calculated as shown in Fig. 5. Figure 5 also shows a typical stress-strain curve. In the figure, the sound velocity increased with strain under elastic regime, and then gradually decreased with increasing plastic strain. In terms of the change in the sound velocity under elastic regime, a linear relation between the sound velocity and the stress was obtained as shown in Fig. 6.

From this relation, the acousto-elastic constant was calculated to be 8.5×10^{-6} MPa^{-1}, which was close to the previous value of 7.8×10^{-6} MPa^{-1} measured in the tensile testing [20] and the value of 8.9×10^{-6} MPa^{-1} measured in the low-cycle fatigue testing [16].

It is well known that the sound velocity changes following change in microstructures. Schmidt et al. [4] examined influence of dislocations on the ultrasonic attenuation and the sound velocity in high purity copper single crystals. Kobayashi et al. [21] measured change in the sound velocity in aluminum alloy with plastic deformation. From these reports, with increasing plastic deformation, the sound velocity decreased due to rotation of crystals (to form the texture), geometric size change and the increase in the dislocation density. In the present work, the cold-rolled specimen was used and the elongation of the specimen was not so large but about 21%. Therefore, influences of the crystallite orientation and the geometric size change on the sound velocity change were not so large, and the sound velocity was mainly affected by increasing the dislocation density confirmed by the surface roughness and the hardness as shown in Fig. 3.

The ultrasonic waves were also measured in real-time during tensile testing. Typical changes in the ultrasonic parameters are shown in Fig. 7. In the figure, the peak intensity and AGTF decreased with increasing strain, and relations of the ultrasonic parameters with strain were in good agreement with those measured off-line with slight difference in the value. However, no change of the peak frequency was obtained.

The deformation of materials causes change in the propagation characteristic of ultrasonic wave due to microstructural evolution. The ultrasonic attenuation appears due to some basic causes [22], such as absorption due to dislocation mobility (described as Granato and Lücke string model), grain boundary scattering and diffraction, and so on. For different materials and testing conditions, changes in the ultrasonic attenuation and the causes may be different. Granato et al. [3] found that the ultrasonic attenuation increased for small deformation to a maximum, and then decreased with further deformation for 2S aluminum. For high purity copper single crystals, Schmidt et al. [4] obtained that the ultrasonic attenuation increased with deformation strain to a maximum, and then decreased and became nearly constant at 5 % strain, and explained the results in terms of dislocation damping theory. Eiras [5] also measured the ultrasonic attenuation for high purity copper single crystals, but only with low deformation between 0.02% and 1% in the <111> direction. Kobayashi et al. [21] used the crystallite orientation distribution function to only explain the sound velocity changes with plastic

deformation for aluminum alloy. Many real-time ultrasonic measurements were developed to evaluate the relation between the ultrasonic attenuation and fatigue cycles in terms of dislocation damping theory [9,11,22], but reports on real-time evaluation of the relation between the ultrasonic attenuation and deformation strain in tensile testing were seldom, especially for aluminum alloy plates A2024-T3. In the present work, for aluminum alloy specimens A2024-T3, changes in the ultrasonic parameters measured in real-time following deformation strain were discussed from evolution of the dislocation density and arrangement, regardless of grain boundary scattering and diffraction due to the smaller elongation of the specimen.

Many studies have discussed on the relation between the deformation process of metals and the ultrasonic attenuation (absorption attenuation) due to interaction of the ultrasonic wave with dislocation mobility [22]. In terms of the Granato and Lücke string model [2,11,23], the ultrasonic attenuation (α) is in proportion to the dislocation density (Λ) and the fourth power of dislocation loop length (L) given by

$$\alpha \propto \Lambda L^4 \tag{1}$$

The peak intensity has a reciprocal relation with the ultrasonic attenuation, and a relation between the gradient of the transfer function $(d\Gamma(\omega)/d\omega)$ and the ultrasonic attenuation constant (δ) is given by [16]

$$\frac{d\Gamma(\omega)}{d\omega} = -\frac{20}{\ln 10}\delta \tag{2}$$

From Eq. (2), AGTF is proportional to the ultrasonic attenuation constant (δ), and when the ultrasonic attenuation is positive $(\delta > 0)$, AGTF is negative.

Relations between the ultrasonic parameters and dislocation structures can be explained as follows. At the initial stage before about 2 % strain of tensile testing as shown in Fig. 7, dislocation density increased due to dislocation multiplication, but dislocation loop length decreased because of tangling among them. In terms of Eqs. (1) and (2), as a result, changes in the peak intensity and AGTF were very small. Following increasing the plastic strain, a large

amounts of dislocations released from their pinning sites and large-scale dislocations movement occurred including development of slip bands. The peak intensity and AGTF gradually decreased due to increase in the dislocation density and loop length. In the subsequent stage after 8 % strain of tensile testing, multiplied dislocations temporarily heavily piled up to obstacles such as grain boundaries, precipitations, and tangled dislocations resulting in less mobility of the dislocations, and then released from the obstacles again. As a result, the peak intensity and AGTF temporarily increased and then decreased again due to change of the mobile dislocations. However, the peak frequency of the bottom echo spectrum was not changed within the accuracy of the present measurement.

3.3 Effect of heat treatment on ultrasonic parameters

When rolled plates are annealed for different annealing times, the initial state of the plate is changed, and recovery, recrystallization and grain growth appear [15]. Figure 8 shows optical micrographs of specimens before and after annealing at 573 K for 2, 4 and 8 hours. Figure 8 (a) shows a typical arrangement of grains observed in as-received state, and the grains elongated in the rolling direction (vertical in the figure). Dark spots in the figure are coarse precipitates. After 2 h annealing (Fig. 8 (b)), fine grains appeared among coarse grains. From rearrangement of grains, it was found that recrystallization occured. Figure 8 (c) shows that the grains became equiaxed, or had approximately same dimensions in all directions. After 8 h annealing (Fig. 8 (d)), the grains became larger due to grain growth. Changes in the Vickers hardness and the yield strength (0.2% offset proof stress) with increasing annealing time were obtained as shown in Fig. 9. In the figure, the hardness continuously decreased with increasing annealing time to 8 h. The yield strength showed a slight increase at an annealing time of 1 h, and then decreased with increasing annealing time to 8 h.

The change in the sound velocity with annealing time is shown in Fig. 10. From the figure, the sound velocity increased at a annealing time of 1 h, and then gradually decreased with increasing annealing time. The increase in the sound velocity was attributed to reduction in the lattice distortion following annihilation of point discontinuities [15]. The decrease in the sound velocity after annealing for 2 h or more was due to rapid decrease in dislocation density

and change in the texture caused by recrystallization confirmed by the mechanical properties and the optical microscope. It was found that the sound velocity measurement as a non-destructive method is a useful tool to distinguish the annealing processes.

The specimens were annealed at 573 K for 2, 4 and 8 hours and subjected to the tensile testing to obtain changes in the ultrasonic parameters with deformation strain measured in real-time. Figure 11 shows typical stress-stain curves of the specimen annealed at 573 K for 0, 2, 4 and 8 hours. The elongations of the annealed specimens were reduced to about a half of that of the as-received specimen. It is well know that the cold-worked metal becomes softer, weaker, yet more ductile after recrystallization. However, decrease in the elongation of the annealed specimens may be attributed to effect of grain boundary precipitation to result in embrittlement occurred [24]. For annealed specimens, the peak intensity and AGTF obtained by the real-time measurement also decreased with increasing plastic strain as shown in Fig. 12. The changes for annealed specimens were also interpreted through changes in the dislocation density and loop length during deformation as well as those for as-received specimen. In the present work, as-received specimen subjected to T3 treatment had a dense dislocation density. After being annealed, the dislocation density of the specimen became lower at the initial state. With increasing annealing time, much lower dislocation density resulted in and rates of the ultrasonic parameters with deformation strain increased as shown in Fig. 13, especially for the gradient of AGTF.

4. Conclusions

By using the local immersion method with a water bag, the real-time ultrasonic measurement was carried out for aluminum alloy specimens A2024-T3 to evaluate the deformation process in the tensile testing, and following conclusions were obtained.

(1) The sound velocity increased with elongation under elastic regime, and then decreased gradually with increasing deformation strain under plastic regime. From the change in the sound velocity with the elastic strain, the acousto-elastic constant was evaluated to be 8.5×10^{-6} MPa^{-1}.

(2) The peak intensity of the bottom echo spectrum and the average gradient of the transfer function obtained from the bottom echo spectrum decreased with increasing plastic strain,

and no change in the peak frequency. The change in the ultrasonic parameters during plastic deformation obtained by the real-time measurement was in good agreement with that measured off-line by the conventional immersion method. The decrease in the ultrasonic parameters was explained from the change in the dislocation density and arrangement by using Granato and Lücke string model.

(3) For annealed specimens, the sound velocity increased after smaller annealing time, and then gradually decreased with increasing annealing time. The peak intensity and AGTF obtained by the real-time measurement also decreased with increasing plastic strain, and the rates of the ultrasonic parameters increased with increasing annealing time.

References

[1] F. Yin, T. Hanamura, O. Umezawa and K. Nagai, Mater. Sci. Eng. A00 (2000) 1-9.

[2] A. Granato and K. Lücke, J. Appl. Phys. 27 (1956) 583-593.

[3] A. Granato, A. Hikata and K. Lücke, Acta. Metall. 6 (1958) 470-480.

[4] H. Schmidt, D. Lenz, E. Drescher and K. Lücke, Journal de Physique (1981) C5: 339-344.

[5] J. A. Eiras, J. Alloys Comp. 310 (2000) 68-71.

[6] W. Johnson, Mater. Sci. Eng. A309-310 (2001) 69-73.

[7] H. Kato, N. Itoi and K. Kageyama, J. Jpn Soc. for Non-Destructive Inspection, 50(1) (2001) 34-40.

[8] L. Shen and H. Kato, NDT&E International 32 (1999) 355-361.

[9] M. Hirao, H. Ogi, N. Suzuki and T. Ohtani, Acta. Mater. 48 (2000) 517-524.

[10] H. Ogi, T. Hamaguchi, M. Hirao, J. Alloys Comp. 310 (2000) 436-439.

[11] S. Kenderian, Tobias P. Berndt, Robert E. Green, Jr, B. Boro Djordjevic, Mater. Sci. Eng. A00 (2002) 1-10.

[12] G. F. Dirras, J. L. Duval and W. Swiatnicki, Mater. Sci. Eng. A263 (1999) 85-95.

[13] Liu Yi-Lin, L. Delaey, E. Aernoudt and O. Arkens, Mater. Sci. Eng., 96 (1987) 125-137.

[14] Liu Yi-Lin, L. Delaey, E. Aernoudt and O. Arkens, Mater. Sci. Eng., 96 (1987) 139-146.

[15] P. Palanichamy and M. Vasudevan, Materials Evaluation, 61(9) (2003) 1020-1025.

[16] X. H. Min and H. Kato, Mater. Sci. Eng. A 372 (1-2) (2004) 269-277.

[17] X. H. Min and H. Kato, Real-time measurement of ultrasonic wave in low-cycle fatigue testing, Proc. Int. Conf. on ATEM, MMD-JSME, Nagoya, Japan, (2003).

[18] X. H. Min, H. Kato, H. Saito and K. Kageyama, J. Jpn Soc. for Non-Destructive Inspection, 52(12) (2003) 697-702.

[19] D. Ye, X. Tong, L. Yao and X. Yin, Mater. Chem. Phy., 56 (1998) 199-204.

[20] M. J. Fisher and G. Herrmann, Acoustoelastic measurements of residual stress, Review of Progress in Quantitative NDE, Vol.3B, D. O. Thompson and D. E. Chimenti, eds., New York, Plenum Press, (1984) 1283-1291.

[21] M. Kobayashi and N. Shimada, Trans. Jpn Soc. Mech. Eng. A 61(590) (1995) 114-120.

[22] H. Ogi And M. Hirao, J. Soc. Mater. Sci., Jpn., 52(3) (2003) 267-272.

[23] H. Ogi, A. Tsujimoto, M. Hirao. H. Ledbetter, Acta. Mater. 47(14) (1999) 3745-3751.

[24] Christian B. Fuller, Albert R. Krause, David C. Dunand and David N. Seidman, Mater. Sci. Eng. A 338 (2002) 8-16.

Captions of the figures

Fig.1 Setup for real-time ultrasonic measurement under tensile testing.
(a) Photograph of setup (b) Schematic representation of setup

Fig.2 Change in ultrasonic parameters with total strain measured by conventional immersion method: (a) relative peak intensity; (b) peak frequency; (c) average gradient of transfer function.

Fig.3 Change in surface roughness (Ra) and Vickers hardness (HV) with total strain.

Fig.4 Change in propagation time and specimen thickness with total strain.

Fig.5 Typical stress-strain curve and change in sound velocity with total strain.

Fig.6 Change in sound velocity with stress under elastic regime.

Fig.7 Change in ultrasonic parameters with total strain measured in real-time during tensile testing: (a) relative peak intensity, (b) peak frequency, (c) average gradient of transfer function.

Fig.8 Optical micrographs: (a) before annealing; (b) annealing for 2 h; (c) annealing for 4 h; (d) annealing for 8 h; The rolling direction is vertical in the figure.

Fig.9 Change in Vickers hardness and yield strength with annealing time.

Fig.10 Change in sound velocity with annealing time.

Fig.11 Typical stress-strain curves after annealing at 573 k for 0, 2, 4 and 8 hours.

Fig.12 Change in ultrasonic parameters after annealing at 573k for 0, 2, 4 and 8 hours with total strain measured in real-time.
(a) Peak intensity (b) Average gradient of transfer function

Fig.13 Change in average gradient of ultrasonic parameters for total strain measured in real-time with annealing time.
(a) Gradient of relative peak intensity (b) Gradient of average gradient of transfer function

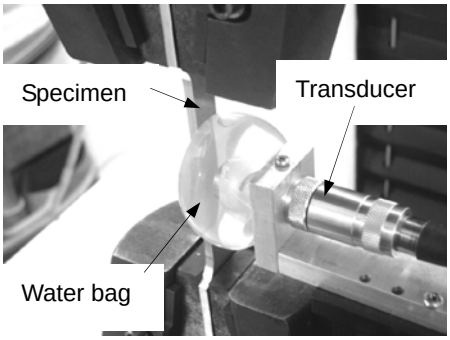

(a) Photograph of setup

Fig.1 Setup for real-time ultrasonic measurement under tensile testing.

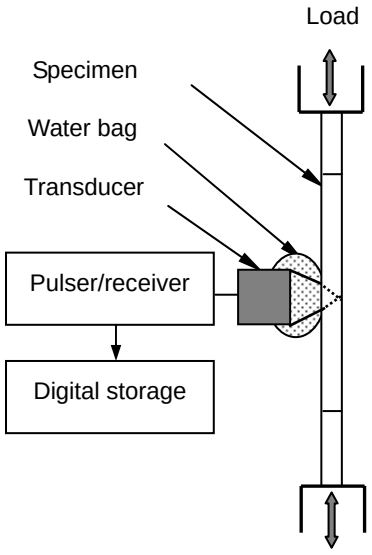

(b) Schematic representation of setup

Fig.1 (continued) Setup for real-time ultrasonic measurement under tensile testing.

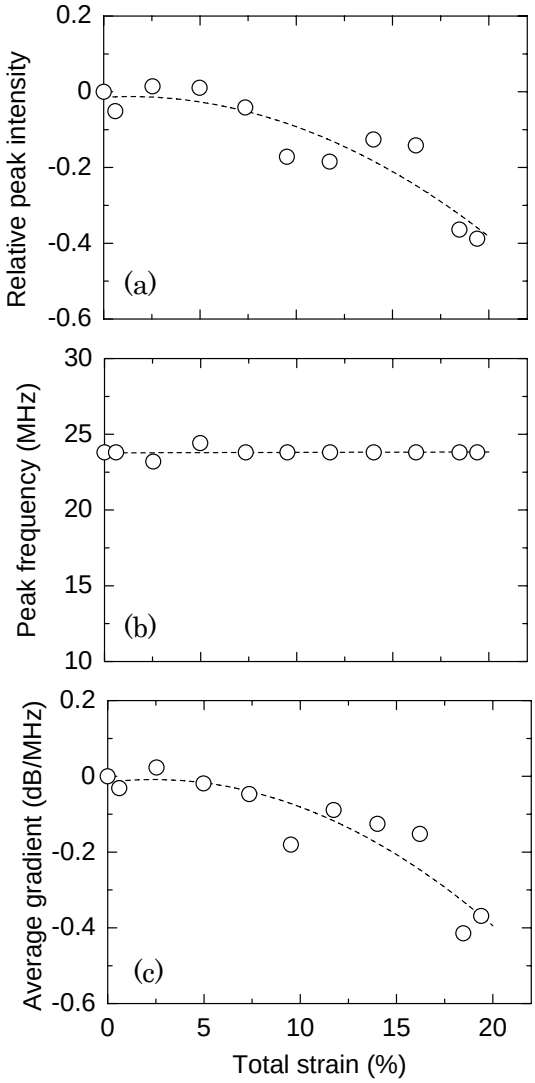

Fig.2 Change in ultrasonic parameters with total strain measured by conventional immersion method: (a) relative peak intensity; (b) peak frequency; (c) average gradient of transfer function.

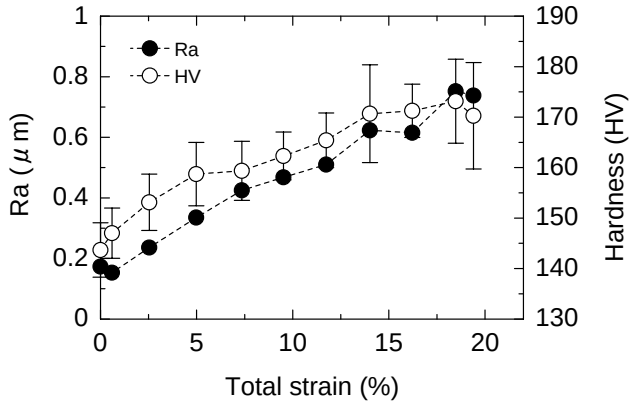

Fig.3 Change in surface roughness (Ra) and Vickers hardness (HV) with total strain.

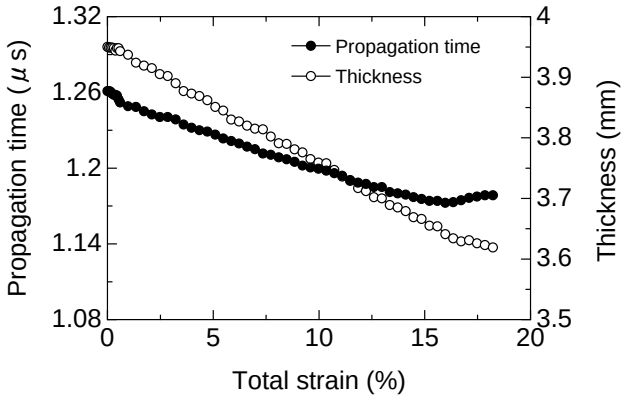

Fig.4 Change in propagation time and specimen thickness with total strain.

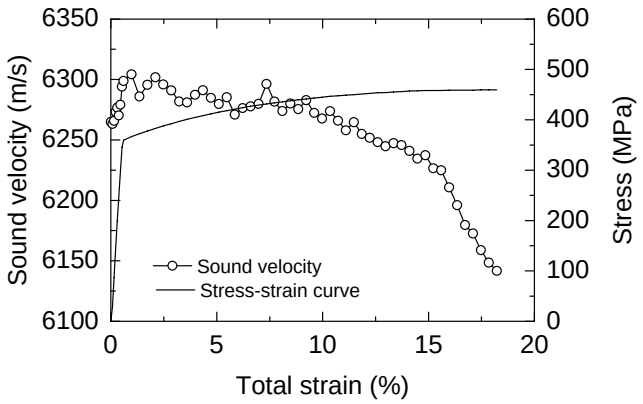

Fig.5 Typical stress-strain curve and change in sound velocity with total strain.

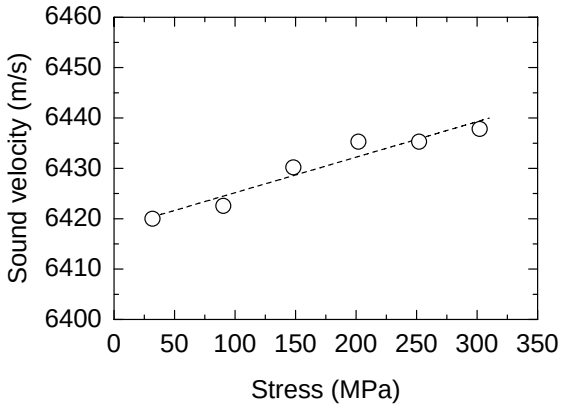

Fig.6 Change in sound velocity with stress under elastic regime.

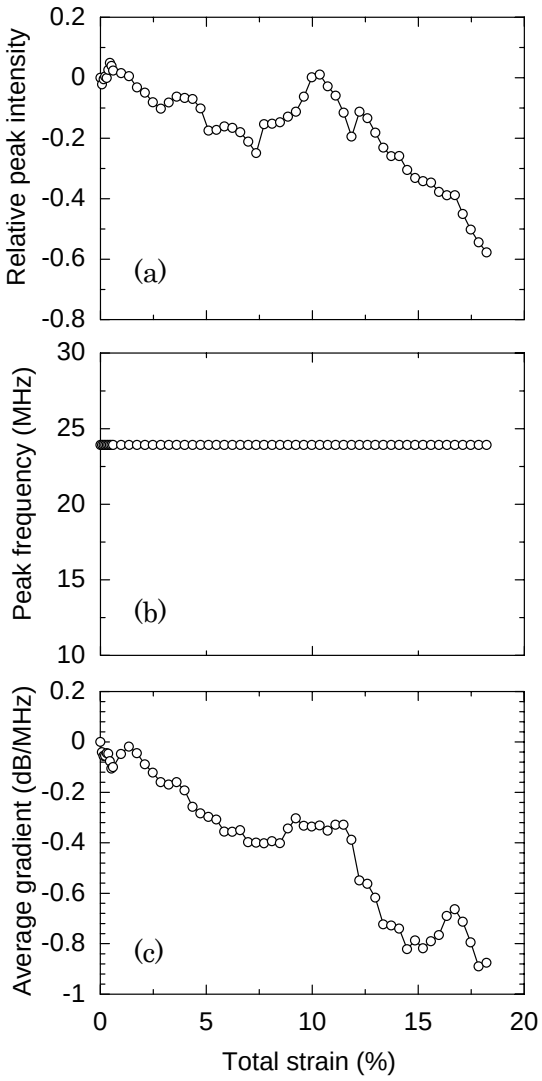

Fig.7 Change in ultrasonic parameters with total strain measured in real-time during tensile testing: (a) relative peak intensity, (b) peak frequency, (c) average gradient of transfer function.

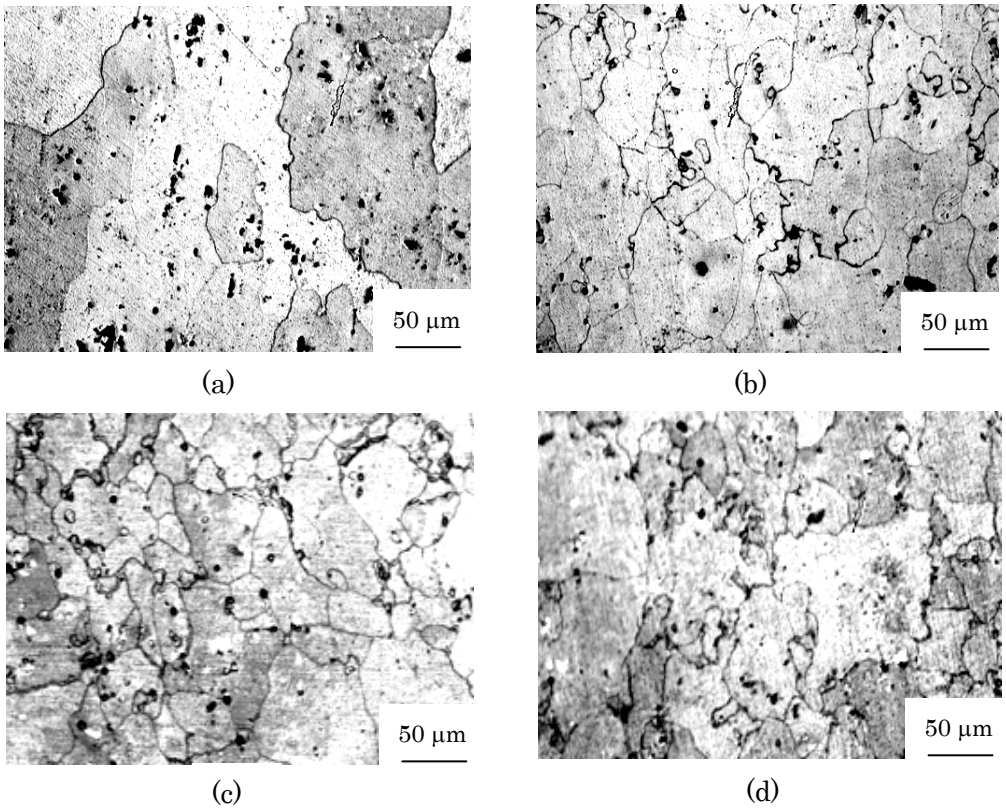

Fig.8 Optical micrographs: (a) before annealing; (b) annealing for 2 h; (c) annealing for 4 h; (d) annealing for 8 h. The rolling direction is vertical in the figure.

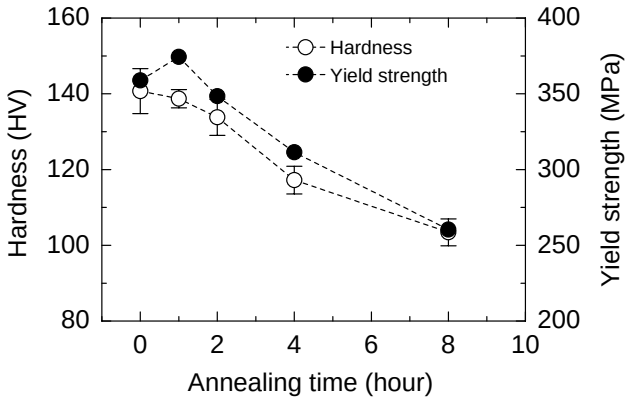

Fig.9 Change in Vickers hardness and yield strength with annealing time.

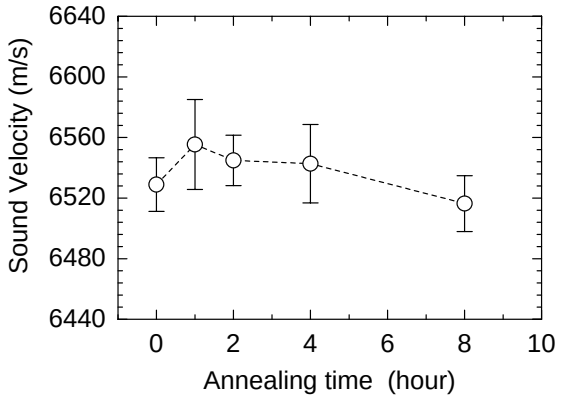

Fig.10 Change in sound velocity with annealing time.

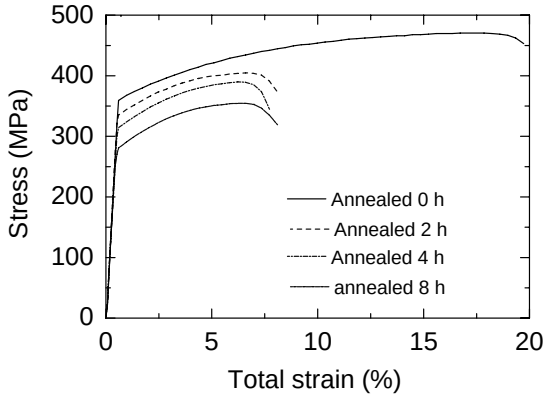

Fig.11 Typical stress-strain curves after annealing at 573 k for 0, 2, 4 and 8 hours.

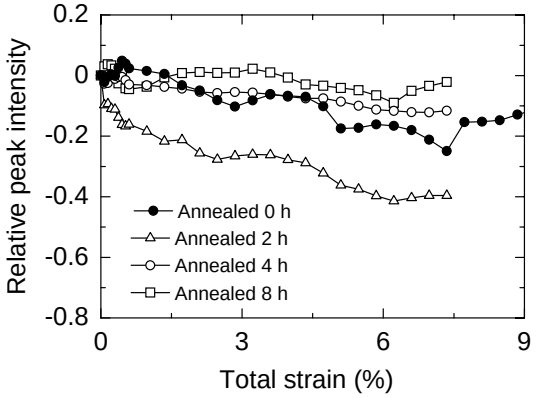

(a) Relative peak intensity

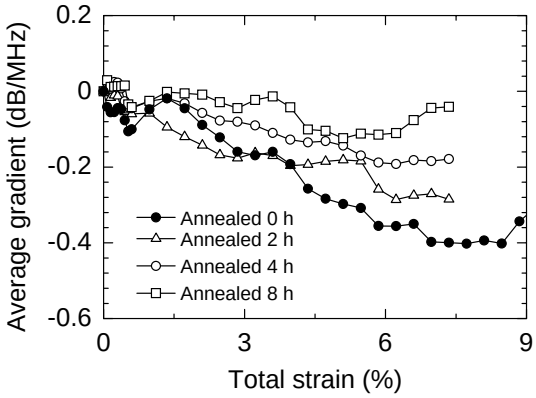

(b) Average gradient of transfer function

Fig.12 Change in ultrasonic parameters after annealing at 573k for 0, 2, 4 and 8 hours with total strain measured in real-time.

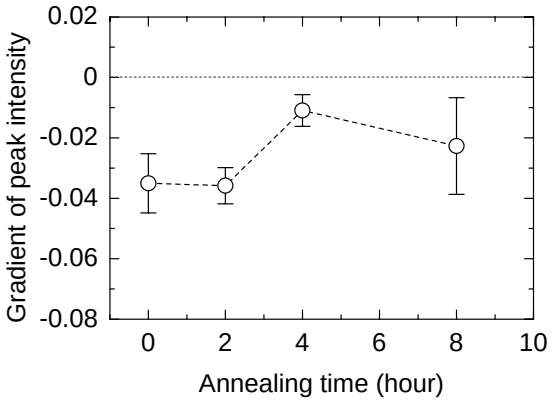

(a) Gradient of relative peak intensity

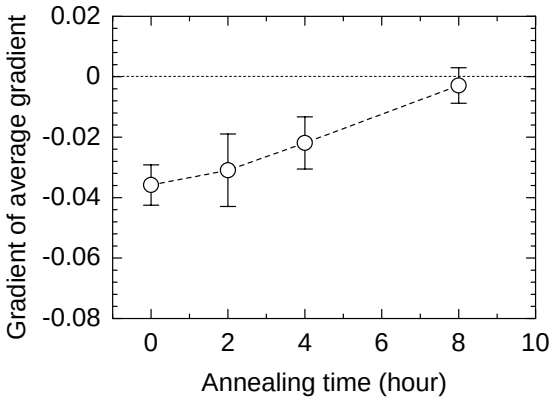

(b) Gradient of average gradient of transfer function

Fig.13 Change in average gradient of ultrasonic parameters for total strain measured in real-time with annealing time.